Towards multiscale modeling of Si nanocrystals LPCVD deposition on SiO2: From ab initio calculations to reactor scale simulations

Ilyes Zahi, Hugues Vergnes, Brigitte Caussat, Alain Estève, Mehdi Djafari Rouhani, Pierre Mur, Philippe Blaise, Emmanuel Scheid

Towards multiscale modeling of Si nanocrystals LPCVD deposition on SiO_2: From ab initio calculations to reactor scale simulations

I. Zahi, H. Vergnes [a], B. Caussat [a,*], A. Estève [b], M. Djafari Rouhani [b], P. Mur [c], P. Blaise [c], E. Scheid [b]

[a] *Laboratoire de Génie Chimique, ENSIACET, Institut National Polytechnique de Toulouse, UMR-CNRS 5503, 5 rue Paulin Talabot, 31106 Toulouse Cedex 1, France*
[b] *Laboratoire d'Analyse et d'Architecture des Systèmes, UPR-CNRS 8011, 7 avenue du Colonel Roche, 31077 Toulouse, France*
[c] *CEA-LETI-MINATEC, 17 avenue des Martyrs, 38054 Grenoble, France*

Abstract

A modeling study is presented involving calculations at continuum and atomistic (DFT, Density Functional Theory) levels so as to better understand mechanisms leading to silicon nanocrystals (NC) nucleation and growth on SiO_2 silicon dioxide surface, by Low Pressure Chemical Vapor Deposition (LPCVD) from silane SiH_4. Calculations at the industrial reactor scale show that a promising way to improve reproducibility and uniformity of NC deposition at short term could be to increase deposition time by highly diluting silane in a carrier gas. This dilution leads to a decrease of silane deposition rate and to a marked increase of the contribution to deposition of unsaturated species such as silylene SiH_2. This result gives importance to our DFT calculations since they reveal that only silylene (and probably other unsaturated species) are involved in the very first steps of nucleation i.e. silicon chemisorption on silanol Si–OH or siloxane Si–O–Si bonds present on SiO_2 substrates. Saturated molecules such as silane could only contribute to NC growth, i.e. chemisorption on already deposited silicon bonds, since their decomposition activation barriers on SiO_2 surface are as high as 3 eV.

Keywords: LPCVD; Nanodots; Silicon; Modelling; DFT; CFD

1. Introduction

The need of high integrated systems (PC, car, MP3, mobile …) of the everyday life involves a permanent evolution of the microelectronic industry. Integrated circuits involving non volatile Flash memories are good examples of these trends since such systems allow the use of very thin tunnel oxides while avoiding leakage current [1,2]. The poly-silicon floating gate of the Flash memories could then be replaced by a discrete trap floating gate in which discrete traps are made up of silicon nanocrystals (NC) [1,2]. The deposition of NC by Low Pressure Chemical Vapor Deposition (LPCVD) from silane SiH_4 on SiO_2 surfaces remains one of the most promising ways of synthesis. Nevertheless, it is mandatory to reach an area density of at least 10^{12} NC/cm^2 and NC radii lower than 5 nm to industrialize convenient and reliable Flash memories. Despite a huge experimental effort, fundamental understanding of the key mechanisms of NC nucleation and growth remains elusive.

The LPCVD process involves well known homogeneous and heterogeneous chemical reactions [3–7]. However kinetic laws for heterogeneous reactions are only established for conventional thick silicon films (i.e. > 50 nm), and Cocheteau et al. [8] have shown that the law of Wilke et al. [7] largely overestimates deposition rate of NC. The reason is that the chemical bonds present on a thermally grown SiO_2 surface (silanol Si–OH and siloxane Si–O–Si bonds, according to Vansant et al. [9]), are much less reactive than fresh silicon dangling bonds. Kinetics of these first deposition steps dominates kinetics of NC formation, such as H_2 desorption from the growing nuclei, which is not the case for thicker films. Moreover, due to low run durations (10 to 30 s) used for NC deposition, discrepancies have been observed leading to poor reproducibility and in addition NC are not deposited uniformly from wafer to wafer on industrial loads involving more than one hundred wafers [8].

* Corresponding author.
E-mail address: Brigitte.Caussat@ensiacet.fr (B. Caussat).

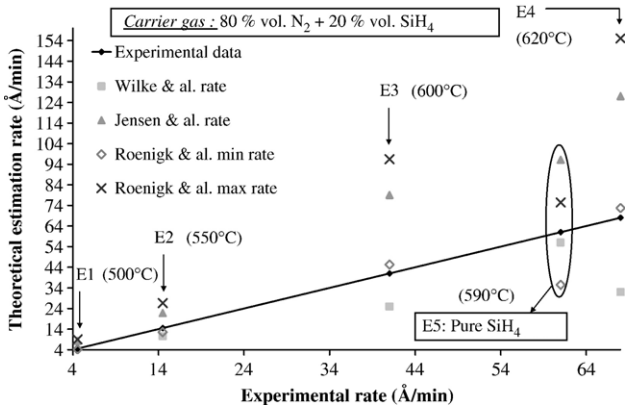

Fig. 1. Comparison between experimental and calculated silicon deposition rates (Å/min), runs E1 to E4 correspond to high dilution conditions and run E5 to pure silane.

In order to study physical and chemical mechanisms existing from NC nucleation toward the industrial process, a multiscale work has been initiated involving respectively first principles calculations for the scale of precursor molecules and surface bonds and the use of computational fluid dynamics (CFD) for the reactor scale, initially addressed in a previous work [10]. To improve reproducibility and uniformity of deposition, we have first investigated by CFD how to decrease deposition rate and thus increase run durations. A promising way of progress at short term could be to highly dilute silane in a carrier gas. By using the CFD code Fluent, the influences of the carrier gas nature (hydrogen or nitrogen) and of the dilution ratio of silane on the deposition rate along the wafer load will be detailed. At the atomistic scale, in order to develop new intrinsic heterogeneous kinetic laws valid for NC deposition, we will detail chemical pathways and associated activation barriers for SiH_2/SiH_4 reactions onto oxide surface species.

2. Experimental

Si NC were synthesized in a Tokyo Electronic Limited (TEL) industrial vertical tubular hot wall LPCVD reactor containing 170 [100] silicon wafers 8′ in diameter as detailed elsewhere [8]. Pure or diluted silane was injected from the bottom part of the reactor and the outlet gas was exhausted by its top part.

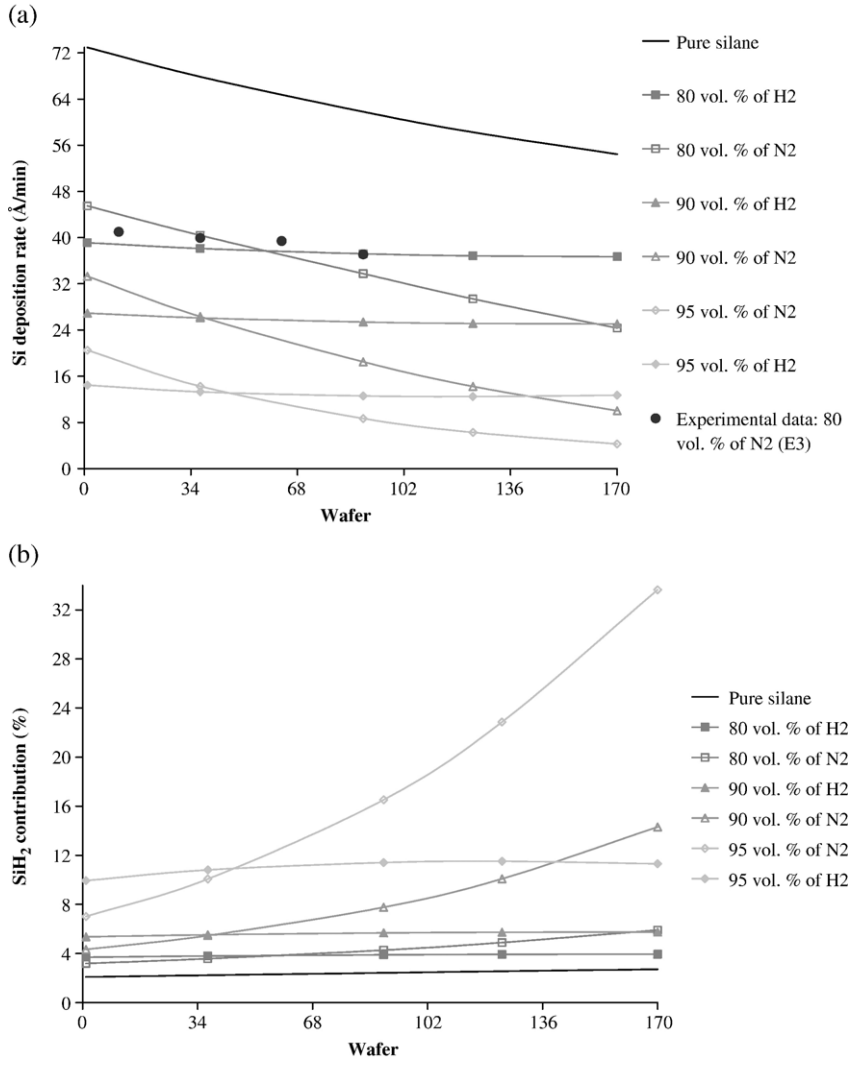

Fig. 2. (a) Silicon deposition rate (Å/min) and (b) contribution to deposition of silylene along the load calculated by Fluent.

Specific experiments have been conducted in order to verify the validity of the heterogeneous kinetic laws of the literature for silicon LPCVD in conditions of high dilution of silane (80 vol.% in N_2). Indeed such conditions of dilution are original and the validity of the few kinetic laws available in the literature remained to be ascertained. Total pressure has been fixed to 0.12 Torr and temperature has been varied between 500 and 620 °C. The targeted thickness was quite high (100 nm) in order to not disturb the results with the substrate influence. For comparison purposes, an experiment (run E5) has been performed using pure silane. Temperatures as low as 500 °C have been studied in order to test also the validity of the kinetic laws in a temperature range quite low for conventional LPCVD but which could be interesting for NC synthesis [11]. Four test wafers have been studied per run, each presenting a SiO_2 layer of 100 nm thick. The deposition rates have been measured by ellipsometry, using the UV1280 spectroscopic ellipsometry from KLA Tencor.

As illustrated in Figs. 1 and 2, we logically observe that deposition rates increase with temperature and decrease along the load and also when silane is diluted.

3. Results and discussion

3.1. Kinetic scheme

Homogeneous and heterogeneous chemical reactions have been considered. We have retained for our operating conditions the homogeneous kinetic laws of Cordier et al. [4] involving only silane SiH_4 and silylene SiH_2 as silicon precursors:

$$SiH_4 \leftrightarrow SiH_2 + H_2 \quad (R1)$$

For this low pressure limit range, these authors proposed non Arrhenius pressure dependant kinetic laws with the following parameters for the forward reaction k_f and for the backward reaction k_b:

$k_f = 7.1 \times 10^7 \times P \times e^{\left(\frac{-197.1\times10^3}{R.T}\right)}$ (s^{-1}) and $k_b = 2 \times 10^2 \times P \times e^{\left(\frac{900}{RT}\right)}$ ($m^3\ mol^{-1}\ s^{-1}$), P corresponding to the total pressure in Pa, and T in K.

Such a simplification of the chemical scheme of silane pyrolysis does not limit the interest of our results because it is well known that in LPCVD conditions, the contribution to deposition of polysilanes of order higher than 2 is negligible and that silylene is among the most concentrated unsaturated species [3,4]. For the heterogeneous reactions, we have considered a Langmuir–Hinshelwood formulation [5–7] for silane decomposition onto surface and kinetic theory for unsaturated species (here silylene) with a sticking coefficient of 1. The corresponding heterogeneous reactions are the following:

$$SiH_4 \rightarrow Si + 2H_2 \quad (R2)$$

$$SiH_2 \rightarrow Si + H_2 \quad (R3)$$

Fig. 1 presents a comparison between experimental deposition rates measured near the gas entrance and calculated ones using three different kinetic laws of the literature for deposition from silane. Note that these calculations have been performed using the inlet partial pressures of silane. The straight line in Fig. 1 corresponds to equality between experimental and theoretical values. Using pure silane, the law of Wilke et al. [7] is the most suitable one to predict deposition rate of conventional thickness as already observed [8]. But in conditions of high dilution of silane, we found that this law under-estimates experimental deposition rates whereas that of Jensen et al [5] over-estimates them. In the opposite, choosing the minimum parameters of the Roenigk et al. law [6] gives agreement with experimental values in high dilution conditions whereas maximum parameters of these authors give the highest over-estimations. It is worth noting that the Roenigk et al. law with its minimum parameters and the Wilke et al. law provide convenient results at temperatures as low as 500 and 550 °C. Thus the Roenigk et al. law with its minimum parameters has been retained to simulate by CFD silicon deposition in high dilution conditions.

3.2. Simulation of the industrial process

Some possible ways of optimization of NC synthesis at short term have been studied by modeling the LPCVD industrial process using the CFD Fluent software (Fluent 6.1.18). We simplified the system by using 2D modeling and we made assumptions of steady state conditions, isothermal reactor, laminar flow, axial symmetry and ideal gas. In these conditions we solved the governing equations of mass, momentum and reactive species transport in order to predict local gas flows, species concentrations and deposition rates everywhere into the reactor. Here the objective was to sharply decrease the total deposition rate while maintaining uniform values along the wafer load, so as to increase deposition duration to values greater than 60 s for NC synthesis. With such run durations, the unsteady regime corresponding to the filling-in of the reactor and to the establishment of reactive mass transfers would become negligible in comparison with the steady state regime [8]. Silane dilution ratios comprised between 80 and 95 vol.% in either H_2 or N_2 have been studied using the law of Roenigk et al. [6] with its minimum parameters as explained in Section 3.1. With this conventional law, an overestimation of NC deposition rates will probably be obtained as explained in introduction, but we only aimed to compare from one simulation to another the influences of carrier gas and dilution ratio on deposition rates along the load. Simulations have been performed for a uniform temperature of 600 °C into the reactor and a total inlet flow rate of 500 sccm.

Total deposition rates along the load calculated by Fluent and also experimentally measured for run E3 (corresponding to 80% dilution of silane in N_2) are presented in Fig. 2(a). Deposition rates are decreased by factors comprised between 1.5 and 12 depending on carrier gases and dilution ratios. For the highest ratio, 95% of silane dilution, the highest decrease of deposition rate is obtained. Due to their different molar weights, hydrogen and nitrogen carrier gases affect more or less diffusion coefficients and then uniformity of deposition rates along the load. Indeed, adding H_2 in the initial mixture involves an important increase of diffusion

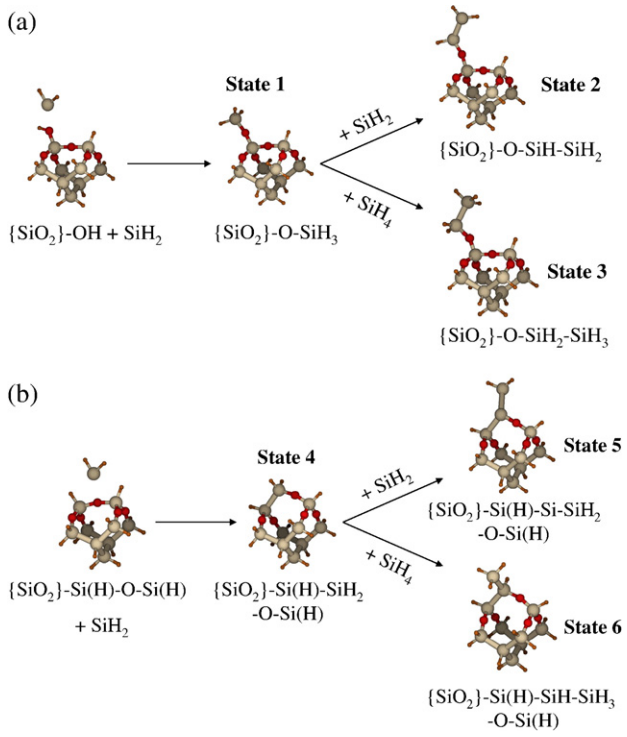

Fig. 3. Structures of the modeled clusters from the initial stage of the reaction to a final stable structure state, (a) from hydroxyl group and (b) from siloxane bridge.

coefficients thus improving deposition uniformity. Using nitrogen or pure silane, the slope of the deposition rate along the load is higher, due to the low coefficients of diffusion involved as represented in Fig. 2(a). Using 95% of silane dilution in H_2 the two objectives of reproducibility and uniformity are reached. Considering the first and last wafers of the load, run duration is increased by a factor 4.8 to 3.8 respectively in comparison with the run performed with pure silane. Experimental deposition rates are in agreement with simulated ones in the case of N_2 as carrier gas with a dilution of 80%.

Contrarily to deposition rates from silane, deposition rates from silylene remain quasi constant whatever the nature of carrier gas and dilution ratio since the concentration of this molecule is nearly the same near surfaces due to its high reactivity. When using pure silane, silylene contribution to deposition is around 2% and silane contributes to the remaining 98% (Fig. 2(b)). When using a silane dilution ratio of 95%, this contribution reaches roughly 10% with H_2 as carrier gas and between 7 and 33% with N_2 from the bottom to the top part of the reactor respectively. These results are important since increasing SiH_2 contribution to deposition could favor nucleation and then increase NC area density as explained below. Once again the use of H_2 provides a better uniformity.

3.3. First principles calculations at the molecular scale

As explained in the introduction section, conventional heterogeneous kinetic laws over-estimate deposition rates in the case of ultrathin Si layers; this requires establishing new kinetic parameters to quantify interactions existing between surface bonds and precursor molecules. This is particularly true at the nucleation step where the complex chemistry taking place at the surface has not yet been fully addressed. To get deeper understanding of the gas/surface interactions, we focus on DFT calculations for evaluation of initial activation barriers and sticking coefficients. We present results dealing with SiH_2 and SiH_4 interactions on simple silanol Si–OH bonds, siloxane Si–O–Si bridged sites and fresh silicon bonds incorporated into SiO_2 surface.

This study has been performed within the framework of Kohn–Sham (KS) density functional theory (DFT), with the gradient corrected hybrid Becke three parameters exchange functional [12] and the Lee–Yang–Parr correlation functional [13] (B3-LYP) as implemented in the Gaussian-03 package [14]. All the atoms are described by the $6-31+G^{**}$ basis set.

Nucleation initiation reactions are presented in Fig. 3 from chemisorption of the precursor molecules on a SiO_2/Si based cluster ($Si_9O_5H_{12}$) up to the final structure; the associated kinetic parameters are given in Table 1. Two substrates are derived from this cluster: $Si_9O_5H_{12}$–H–OH and $Si_9O_5H_{14}$ corresponding to the hydroxyl sites (OH) and siloxane bridges (Si–O–Si), respectively. Kinetic parameters such as sticking coefficients, activation barriers, adsorption energies and formation energies indicating if the reaction is exothermic or endothermic, have then been evaluated as detailed in Table 1. Calculations indicate that the very first step of NC nucleation

Table 1
Kinetic parameters for SiH_2/SiH_4 interactions with SiO_2 surface sites and chemisorbed silicon, obtained from DFT results

Calculations on SiO_2 cluster		Activation barrier (eV)	Adsorption energy (eV)	Formation energy (eV)	Sticking coefficient	
Precursor	Surface site				SiH_2	SiH_4
SiH_2 (State 1)	Si–OH	0.88	0.61	−2.59	0.027	
SiH_2 (State 2)	Si–H	0	2.06	−2.06	1	
SiH_4 (State 3)	Si–H	0.44	0.01	−1.74		0.003
SiH_2 (State 4)	Si–O–Si	0.65	0.27	−1.54	0.006	
SiH_2 (State 5)	Si– (dangling bond)	0	2.26	−2.26	1	
SiH_4 (State 6)	Si– (dangling bond)	0.29	0.007	−1.79		0.021
SiH_4	Si–OH	3	0.03	−0.61		$\sim 5.3.10^{-18}$
SiH_4	Si–O–Si	3	0.006	+0.75 (endothermic)		$\sim 5.2.10^{-18}$
H_2	Desorption (State 1)	2.76	−2.05	+2.04 (endothermic)		
H_2	Desorption (State 4)	2.37	−2.18	+2.14 (endothermic)		

could only proceed from unsaturated species chemisorption with activation energies of 0.88 eV (state 1 Fig. 3(a)) and 0.65 eV (state 4 Fig. 3(b)) onto hydroxyl groups and siloxane bridges respectively. Energies involved in physisorption and decomposition reactions of SiH_4 on both silica surface sites are highly unfavorable for creating direct silicon incorporation. However SiH_4 could contribute to NC second step nucleation, i.e. to silicon chemisorption on already deposited silicon atoms (state 3 and state 6 in Fig. 3 (a) and (b) respectively). For the first step of nucleation, we found very low sticking coefficients for SiH_4 and SiH_2 onto SiO_2 surface species, see Table 1. These sticking coefficients have been calculated at 873 K, for conditions corresponding to our CFD simulations, by the use of a total accumulation regime formulation for SiH_4 first step nucleation and a depletion regime formulation for SiH_2 and SiH_4 further step nucleation.

The sticking coefficient was calculated from the reaction and desorption fluxes respectively J_r and J_d. The expression is as follow:

$$\gamma = \frac{J_r}{J_d + J_r}, \text{ for the depletion regime.}$$

Concerning the H_2 desorption mechanism from state 1 and 4, we found desorption energies as high as 2.76 and 2.37 eV respectively, in agreement with values from the literature [15–17]. After this desorption mechanism, SiH_4 and SiH_2 could easily nucleate on surface species presenting dangling bonds. Thus sticking coefficients for the two precursors became much higher. The important point is that for these first reactions of deposition on SiO_2, H_2 desorption will be an important limiting step.

4. Conclusion

Fluent simulations indicate that by diluting at 95 vol.% silane in nitrogen, the deposition time could be increased by a factor 4. In addition, silylene contribution to deposition could reach between 7 and 33% using N_2 as carrier gas, instead of 2% when using pure silane. This result gives importance to first DFT calculations since they show that the first insertion of silicon on silanol or siloxane bonds present on SiO_2 surface sites could only proceed from silylene (and probably from other unsaturated species). Increasing silylene contribution to deposition in highly diluting silane could then exalt silicon nucleation and then NC density probably in lowering their size. Further works are in progress to complete our chemical mechanism for silane pyrolysis and analyze by DFT the interaction of the various precursors with the surface sites. The final objective is to implement in the CFD code at the reactor scale, intrinsic kinetics of these first steps reactions obtained from DFT results so as to reach a better mastery of the NC features, i.e. density and size.

Acknowledgement

We wish to thank CALMIP supercomputer centers for computer resources and CNRS/CEA-LETI-MINATEC for financial support.

References

[1] S. Tiwari, F. Rana, K. Chan, H. Hanafi, W. Chan, D. Bucanan, Appl. Phys. Lett. 68 (1996) 1377.
[2] J. DeBlauwe, IEEE Trans. Nanotechnol. 1 (2002) 72.
[3] C.R. Kleijn, J. Electrochem. Soc. 138 (7) (1991) 2190.
[4] C. Cordier, E. Dehan, E. Scheid, P. Duverneuil, Mat. Sci. Eng. B, 37 (1996) 30.
[5] K.F. Jensen, D.B. Graves, J. Electrochem. Soc. 130 (1983) 1950.
[6] K.F. Roenigk, K.F. Jensen, J. Electrochem. Soc. 132 (1985) 448.
[7] T.E. Wilke, K.A. Turner, C.G. Takoudis, Chem. Eng. Sci. 41 (4) (1986) 643.
[8] V. Cocheteau, B. Caussat, P. Mur, E. Scheid, P. Donnadieu, T. Billon, Electrochem. Soc. Proc. 2005-09, 2005, p. 523.
[9] E.F. Vansant, P. Van Der Voort, K.C. Vrancken, Stud. Surf. Sci. Catal. 93 (1995).
[10] I. Zahi, H. Vergnes, B. Caussat, A. Esteve, M. Djafari Rouhani, P. Mur, Ph. Blaise, E. Scheid, Mater. Res. Soc. Symp. Proc. 959 (2007).
[11] T. Baron, F. Mazen, J.M. Hartmann, P. Mur, R.A. Puglisi, S. Lombardo, G. Ammendola, C. Gerardi, Solid-State Electron. 48 (2004) 1503.
[12] A.D. Becke, J. Chem. Phys. 98 (1993) 5648.
[13] C.T. Lee, W.T. Yang, R.G. Parr, Phys. Rev., B 37 (1988) 785.
[14] M.J. Frisch, G.W. Trucks, H.B. Schlegel, G.E. Scuseria, M.A. Robb, J.R. Cheeseman, J.A. Montgomery Jr., T. Vreven, K.N. Kudin, J.C. Burant, J.M. Millam, S.S. Iyengar, J. Tomasi, V. Barone, B. Mennucci, M. Cossi, G. Scalmani, N. Rega, G.A. Petersson, H. Nakatsuji, M. Hada, M. Ehara, K. Toyota, R. Fukuda, J. Hasegawa, M. Ishida, T. Nakajima, Y. Honda, O. Kitao, H. Nakai, M. Klene, X. Li, J.E. Knox, H.P. Hratchian, J.B. Cross, C. Adamo, J. Jaramillo, R. Gomperts, R.E. Stratmann, O. Yazyev, A.J. Austin, R. Cammi, C. Pomelli, J.W. Ochterski, P.Y. Ayala, K. Morokuma, G.A. Voth, P. Salvador, J.J. Dannenberg, V.G. Zakrzewski, S. Dapprich, A.D. Daniels, M.C. Strain, O. Farkas, D.K. Malick, A.D. Rabuck, K. Raghavachari, J.B. Foresman, J.V. Ortiz, Q. Cui, A.G. Baboul, S. Clifford, J. Cioslowski, B.B. Stefanov, G. Liu, A. Liashenko, P. Piskorz, I. Komaromi, R.L. Martin, D.J. Fox, T. Keith, M.A. Al-Laham, C.Y. Peng, A. Nanayakkara, M. Challacombe, P.M.W. Gill, B. Johnson, W. Chen, M.W. Wong, C. Gonzalez, J.A. Pople, Gaussian 03, Revision B.05, Gaussian, Inc., Pittsburgh PA, 2003.
[15] C.M. Greenlief, M. Armstrong, J. Vac. Sci. Technol., B 13 (1995) 1810.
[16] L.A. Okada, M.L. Wise, S.M. George, Appl. Surf. Sci. 82/83 (1994) 410.
[17] C.M. Greenlief, M. Liehr, Appl. Phys. Lett. 64 (1994) 601.